Human ornithine transcarbamylase: crystallographic insights into substrate recognition and conformational changes

Dashuang SHI*[1], Hiroki MORIZONO*, Xiaolin YU*, Liang TONG†, Norma M. ALLEWELL‡ and Mendel TUCHMAN*

*Children's National Medical Center, 111 Michigan Avenue, Washington, DC 20010, U.S.A., †Department of Biological Sciences, 1212 Amsterdam Avenue, Colombia University, New York, NY 10027, U.S.A., and ‡College of Life Science, 2300 Symons Hall, University of Maryland, College Park, MD 20742, U.S.A.

Two crystal structures of human ornithine transcarbamylase (OTCase) complexed with the substrate carbamoyl phosphate (CP) have been solved. One structure, whose crystals were prepared by substituting *N*-phosphonacetyl-L-ornithine (PALO) liganded crystals with CP, has been refined at 2.4 Å (1 Å = 0.1 nm) resolution to a crystallographic *R* factor of 18.4%. The second structure, whose crystals were prepared by co-crystallization with CP, has been refined at 2.6 Å resolution to a crystallographic *R* factor of 20.2%. These structures provide important new insights into substrate recognition and ligand-induced conformational changes. Comparison of these structures with the structures of OTCase complexed with the bisubstrate analogue PALO or CP and L-norvaline reveals that binding of the first substrate, CP, induces a global conformational change involving relative domain movement, whereas the binding of the second substrate brings the flexible SMG loop, which is equivalent to the 240s loop in aspartate transcarbamylase, into the active site. The model reveals structural features that define the substrate specificity of the enzyme and that regulate the order of binding and release of products.

Key words: carbamoyltransferase, crystal structure, domain movement, substrate recognition.

INTRODUCTION

Human ornithine transcarbamylase (OTCase) is a member of the transcarbamylase family. This group of proteins includes aspartate transcarbamylase (ATCase; EC 2.1.3.2), OTCase (EC 2.1.3.3), oxamate transcarbamylase (EC 2.1.3.5) [1,2], putrescine transcarbamylase (EC 2.1.3.6) [3,4] and the putative lysine transcarbamylase (EC 2.1.3.8) [5,6]. These enzymes share a common biological function; to transfer a carbamoyl group from carbamoyl phosphate (CP) to an amino group of the second substrate. ATCase, in which the second substrate is L-aspartate, and OTCase, in which L-ornithine is the second substrate, are the two best studied proteins in this family [7,8]. Whereas ATCase has been widely used as a model system for understanding how protein–protein interactions mediate signal transduction, several OTCase crystal structures, which have been solved recently, provide important insights into the folding of the polypeptide chain and the catalytic mechanism of this enzyme [9–14].

There are two kinds of OTCase enzymes, anabolic and catabolic. Anabolic OTCase catalyses the formation of citrulline and phosphate from L-ornithine and CP in the urea cycle or in the biosynthesis of arginine. Anabolic OTCases usually occur as trimeric molecules with subunits of 35–40 kDa in molecular mass, but the anabolic OTCase from *Pyrococcus furiosus*, a thermophilic archaebacterium, is a dodecamer. Catabolic OTCases are part of the catabolic arginine deiminase pathway, and catalyse the formation of CP and L-ornithine from citrulline and phosphate. They are usually larger than anabolic OTCases with 12 identical subunits in the holoenzyme and display pronounced allosteric behaviour [11,15].

The recent crystal structure determinations of unliganded catabolic *Pseudomonas aeruginosa* OTCase and anabolic *Py. furiosus* OTCase [11,12], unliganded and *N*-(phosphonacetyl)-L-ornithine (PALO)-liganded anabolic *Escherichia coli* OTCase [9,10] and PALO-liganded human OTCase [13], indicate that all of the enzymes have similar tertiary structures, which are similar to the catalytic subunit of ATCase. Each subunit has a bilobal structure with the CP binding pocket at the base of the cleft between the two lobes and the L-ornithine binding pocket at the edge of the cleft. The SMG loop (residues 263–286 in human OTCase), which is equivalent to the 240s loop in *E. coli* ATCase and contains an invariant Ser-Met-Gly motif in all OTCases, swings towards the active site to cover the cleft and interacts with the second substrate when both substrates bind. Structural comparisons between OTCase and ATCase indicate that their common substrate, CP, binds to both enzymes in a similar way, consistent with strong sequence similarity of the N-terminal portions. Molecular recognition of the second substrate seems to rely on structural differences in the C-terminal portion, especially the differences in their SMG/240s loops.

We have previously reported the crystal structures of human and *E. coli* OTCase complexed with the bisubstrate analogue PALO, and the ternary complex of human OTCase bound to CP and L-norvaline [10,13,14]. These structures indicate that binding of the bisubstrate analogue or both substrates results in closure of the two domains and movement of the SMG loop. This conformational change is similar to that which occurs in ATCase when *N*-phosphonacetyl-L-aspartate binds to the catalytic subunit of the enzyme [16]. However, differential ultraviolet absorption experiments show that binding of the first substrate,

Abbreviations used: ATCase, aspartate transcarbamylase; CP, carbamoyl phosphate; OTCase, ornithine transcarbamylase; PALO, *N*-phosphonacetyl-L-ornithine; RMSD, root-mean-square deviation.

[1] To whom correspondence should be addressed (e-mail dshi@childrens-research.org).

Atomic coordinates and structural factors (codes 1EP9 and 1FVO respectively) have been deposited in the Protein Data Bank, Research Collaboratory for Structural Bioinformatics, Rutgers University, New Brunswick, NJ, U.S.A.

CP, to *E. coli* or human OTCase induces most of the conformational change [17,18], in contrast with ATCase where the ultraviolet absorbance change does not occur until the second substrate, L-aspartate, binds [19]. In order to clarify the role of CP in inducing the conformational changes and fully understand substrate recognition by the enzyme, it was important to determine the structures of the binary complex of the enzyme with the first substrate bound. In the present study we have determined the structures of the binary complex of human OTCase with CP at 2.4 and 2.6 Å (1 Å = 0.1 nm) resolution, using crystals from different preparation methods. These structures represent an intermediate stage between the apo-enzyme and the ternary complex of the enzyme, and allow us to dissect more precisely the specific substrate-induced conformational changes of the enzyme during the catalytic reaction.

MATERIALS AND METHODS

Crystallization

Human wild-type recombinant OTCase was prepared, purified and stored as previously described [20]. PALO was synthesized by Drs G. Barany and D. Venugopal (Department of Chemistry, University of Minnesota, MN, U.S.A.) as described by Morizono et al. [20]. The first binary complex crystals were prepared by soaking PALO-liganded crystals, which were grown as previously described [13], with a 100 mM CP solution. PALO is a reversible inhibitor, which can be displaced by CP concentrations as low as 10 mM, demonstrated when affinity chromatography is used to purify the enzyme [20]. Ligand exchange was accomplished by transferring the crystals with a loop to a fresh solution of CP every 2 h seven times. This procedure ensured that virtually all of the PALO was replaced by substrate, as has been observed in the preparation of the ternary complex [14]. The second binary complex crystals were obtained by mixing equal amounts (8 μl) of protein solution and reservoir solution [0.1 M MES (pH 6.5) containing 16 % (w/v) poly(ethylene glycol) 8000]. The resulting crystal structure indicated that significant electron density, which can readily be modelled as CP, is present in the same position as that seen for the first binary complex. To our surprise, CP, which was used to elute protein from a PALO affinity column, seems to be trapped in a stable form in the enzyme for several weeks. Therefore this structure is essentially the structure of a CP-liganded binary complex.

Table 1 Crystallographic data and refinement statistics

Parameter	Data	
Space group	$P2_13$	$I23$
Cell dimensions (Å)	$a = b = c = 125.60$	$a = b = c = 203.43$
Resolution limits (Å)	20–2.4	30–2.6
Number of reflections (unique)	333653 (26061)	300506 (42459)
R_{merge} (%)	11.1 (40.2)*	10.8 (26.8)*
$\langle I \rangle / \sigma$	23.3 (3.2)*	6.8 (2.9)*
Number of atoms in final model	2695	5133
Number of reflections involved in refinement	21001 (1884)*	41624 (6338)*
R value (%)	18.4 (21.9)*	20.2 (30.4)*
R_{free} value (%)	22.3 (27.1)*	23.6 (31.8)
RMSD ideal bond length (Å)	0.011	0.006
RMSD ideal bond angle (°)	2.6	1.3
RMSD ideal dihedral angle (°)	24.0	23.1

* Statistics in parentheses are for the highest resolution shell.

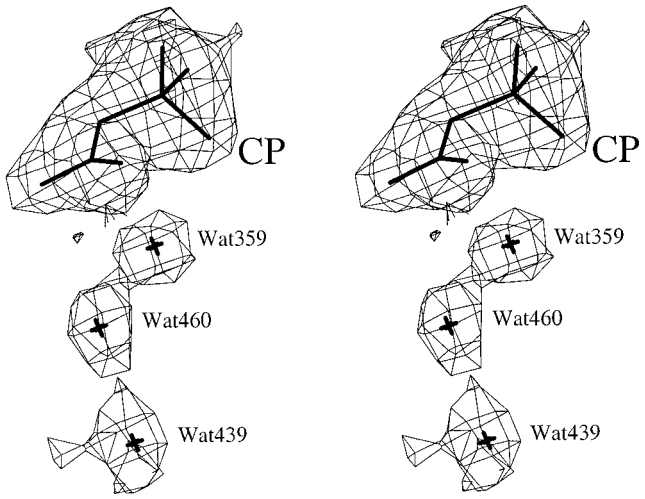

Figure 1 $2|F_o|-|F_c|$ electron density map (contour at 1σ) around CP and three water molecules after refinement

The conformations of CP are unambiguously defined. Wat, water.

Data collection

The data for the PALO-replaced binary complex were collected at 80 K using a Rigaku rotating anode X-ray generator with focus mirror and Siemens area detector. The data were subsequently processed with XENGEN [21]. Crystals were soaked in a solution containing 30 % (v/v) glycerol for a few seconds, and were cryo-cooled with liquid nitrogen before mounting. The data for the CP-cocrystallized binary complex were collected at room temperature on a MAR Research 30 cm image-plate detector at beam line X12B at National Synchroton Light Source. Due to the rapid decay of diffraction under the synchrotron source four crystals were used for the data collection. The data were processed using DENZO and SCALPACK [22]. Data collection statistics are given in Table 1.

Structure determination

The crystal structures of the PALO-replaced binary complexes are isomorphous to the PALO-liganded structure. Following 15 cycles of rigid-body refinement using the PALO-complexed structure with PALO and solvent omitted as the starting model, the electron density of CP was visible in the $|F_o|-|F_c|$ and $2|F_o|-|F_c|$ maps (Figure 1). The carbamoyl plane of CP was well defined and ligands were built into the structure using the graphics program O [23]. The density for the first two residues and residues 267–276 in the SMG loop is weak, but the main chain of the SMG loop is easily traced.

The resulting model was refined with the program XPLOR [24], and higher resolution data were gradually added until all reflections were included. Low resolution data were included after the bulk solvent correction was applied [25]. Individual isotropic B values were refined and solvent molecules were added when the phases had been extended to the highest resolution. Water molecules were identified as peaks of well defined electron density in $|F_o|-|F_c|$ ($> 3\sigma$) and $2|F_o|-|F_c|$ maps ($> 1\sigma$) using the CCP4 programs PEAKMAX [26] and O [23]. All water molecules formed at least one hydrogen bond to protein or other well-established water molecules. In total, 159 water molecules were included in the final model of the binary complex.

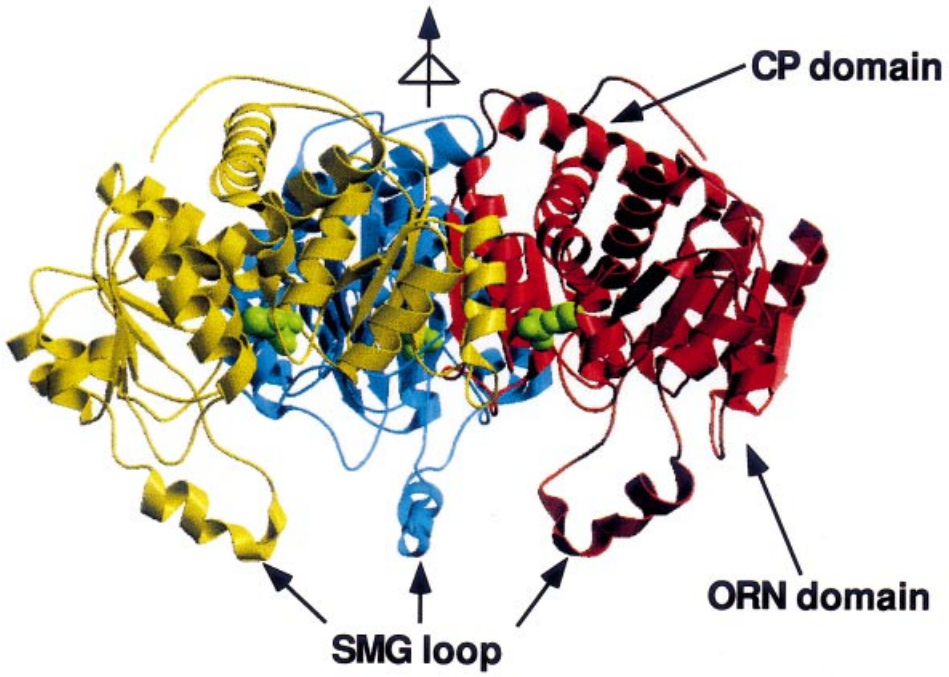

Figure 2 Ribbon representation of the OTCase trimer. The three monomers are coloured blue, red and yellow

The CP molecules are shown as space-filling models coloured green. The ribbon trace was generated with the program MOLSCRIPT [58] and Raster3D [59,60]. Abbreviation used: ORN, L-ornithine.

During the refinement, the same randomly selected set of 10% reflections from various resolution bins, which were not included in the refinement, was used to calculate R_{free} in order to monitor the progress of refinement [27]. The program PROCHECK [28] was used to confirm the accuracy of the structure: 88.4% of ϕ and Ψ values are located in the most favoured regions in the Ramachandran plot. The unusual torsional angles of two outliers, Leu^{163} and Leu^{304}, have been rationalized in terms of their structural and functional roles [13]. The average temperature factors for backbone, side chains, ligand and 159 solvent atoms were 22.26, 24.50, 13.78 and 25.40 Å^2 respectively.

The crystals of the CP-cocrystallized binary complex were in space group $I23$ with cell dimensions $a = b = c = 203.43$ Å. The structure was solved by the combined molecular replacement protocol [29,30] with the program *COMO* (L. Tong, unpublished work) and the PALO-liganded human OTCase structure as a search model. Two monomers were present in an asymmetric unit. The catalytic trimers were generated using the crystallographic 3-fold axis. The refinement of atomic positions and B factors was carried out using the program CNS, version 1.0 [31]. Reflections (5%) from various resolution bins were set aside to monitor the progress of refinement. The initial structural model after rigid-body refinement was subjected to 600 steps of torsional-angle molecular dynamics with a starting temperature of 2500 K to reduce R to 27.5% and R_{free} to 32.2% using all data up to 2.6 Å. At this stage, the model was adjusted using the program O. The electron density of CP was visible in the $2|F_o|-|F_c|$ maps and a model of CP was built. The SMG loop was easily re-built for one of the monomers, but the electron density of the SMG loop for the other monomer was weak. Further refinement using all data to 2.6 Å reduced R to 21.3% and R_{free} to 24.1%. Water molecules were added using the CNS water pickup protocol. A water molecule was picked up if it was $> 3.5\sigma$ in the $|F_o|-|F_c|$ map and made at least one hydrogen bonding contact that was less than 3.5 Å. In total, 44 water molecules were added. The final refinement resulted in an R value of 20.2% and an R_{free} of 23.6%. The average temperature factor for all atoms is 52.0 Å^3, which compares well with that of 50.0 Å^3 from the Wilson plot. The temperature factors for CP are high, implying there is only partial occupancy of CP in the active site. The final refinement statistics are listed in Table 1.

RESULTS

Comparison between two binary complex structures

The two monomers in the CP-cocrystallized binary structure are closely related, superposing with a root-mean-square deviation (RMSD) of 0.33 Å for 321 equivalent C$^\alpha$ atoms. Even though the crystals are prepared differently, the structures of the PALO-replaced and the CP-cocrystallized binary complex are also closely related with an RMSD of approx. 0.43 Å for 311 equivalent C$^\alpha$ positions excluding part of the SMG loop (residues 267–277). Therefore the structure of the PALO-replaced binary complex is a good model of the CP-liganded complex. Since the structure of the PALO-replaced binary complex was refined to slightly higher resolution, the CP is in higher occupancy, and the two structures are very similar, the Results and Discussion sections are mainly based on the structure of the PALO-replaced binary complex.

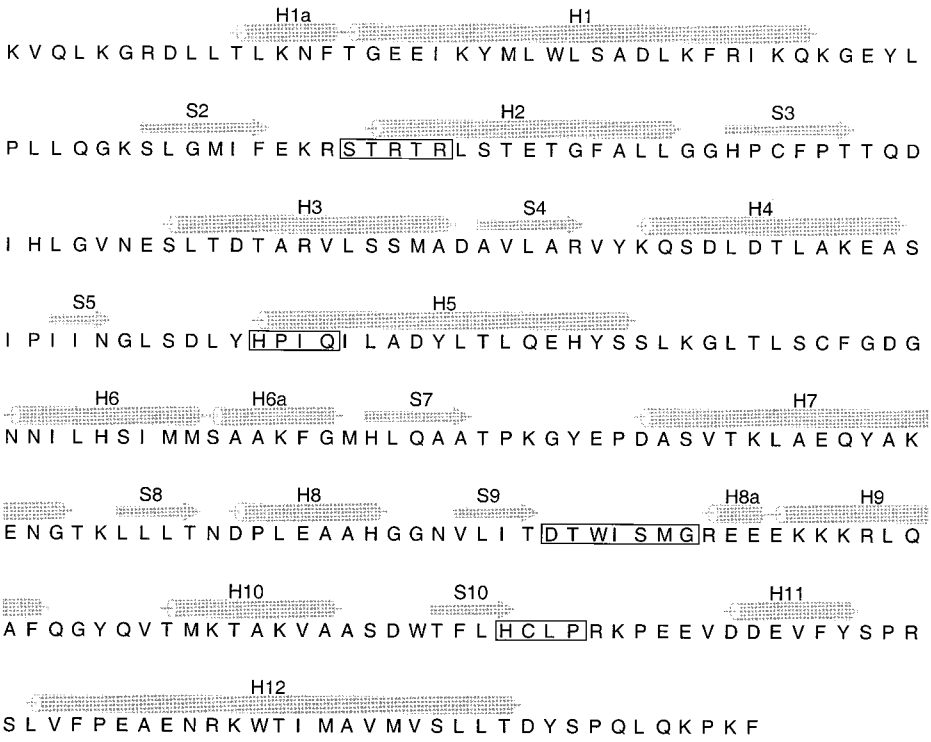

Figure 3 Human OTCase sequence with the secondary structure calculated by the program PROMOTIF [32]

The conserved motifs that are discussed in the text are shown in boxes. The helices are denoted by 'H'; the strands are shown by 'S' (the 'a' suffix was added to keep the overall numbering of the major helices and strands the same across different OTCases and ATCases). H10, H11 and H12 were named H9, H10 and H11 in the previous paper [13]. The Figure was generated using the program ALSCRIPT [61].

Overview of the structure

The enzyme is a trimer of exact 3-fold symmetry with one active site/monomer (Figure 2). Each polypeptide chain folds into two structural domains, linked by two long interdomain helices (helix 5 and helix 12), and each domain has a central parallel β-sheet surrounded by α-helices and loops with α/β topology. The secondary structure, calculated by the program PROMOTIF [32], is illustrated in Figure 3. The active site is located in the cleft between the two domains and is shared by adjacent monomers. The conserved Ser-Thr-Arg-Thr-Arg (residues 90–94) and His-Pro-Xaa-Gln (residues 168–171) motifs, which bind CP, are located at the N-terminal ends of helix 2 and helix 5 respectively. The overall structure of the CP-liganded enzyme is very similar to that of PALO-liganded and CP-L-norvaline-liganded OTCase [13,14]. The relative position of the two domains in the binary complex is similar to that in the CP-L-norvaline-liganded ternary complex with an RMSD of 0.36 Å for 311 equivalent C^{α} positions, excluding part of the SMG loop (residues 267–277). The most significant structural difference between the CP-liganded complex and the CP-L-norvaline-liganded and PALO-liganded complexes is that the SMG loop is displaced from the active site and is less ordered. The conformation of the 'adjacent loop', which is equivalent to the 80s loop in ATCase and contributes a residue (His^{117} in human OTCase) that binds CP from an adjacent subunit, is also significantly different in the CP-liganded binary complex and the CP-L-norvaline-liganded ternary complex. The maximum shift is 3.1 Å for the C^{α} atom of Val^{120}. The superposition of the binary and ternary structures is shown in Figure 4(A).

Active site

The residues that are involved in binding CP are shown in Figure 5 and are listed in Table 2. The CP binding site in the binary complex is similar to that in the ternary complex [14]. Ser^{90}, Thr^{91}, Arg^{92}, Thr^{93} and Arg^{141} from one subunit and His^{117} from the adjacent subunit are involved in binding the phosphate group of CP. Gln^{171}, Cys^{303} and Arg^{330} are involved in the interaction with the primary nitrogen of CP. Thr^{93}, Arg^{141} and His^{168} are involved in binding the carbonyl oxygen of CP.

In the PALO-replaced binary complex crystal, because of the absence of the second substrate, three new water molecules, water-359, water-460 and water-439, fill the L-ornithine binding site (Figure 6). These water molecules are discussed in more detail in the following section.

Solvent structure around the active site

In the binary structure, because of the absence of the second substrate, the water molecule that links the side chain of Lys^{88} and the second substrate is not present. However, the side chain of Lys^{88}, which interacts with Asp^{165}, has the same conformation in the binary structure as in the ternary structure. This highly conserved Lys^{88}, whose conformation is maintained through an interaction with residue 165 (aspartic acid or asparagine), seems to be one of the key residues involved in binding the second substrate via a water molecule. Chemical modification of this lysine results in complete loss of enzyme activity [33]. As noted above, three new water molecules, water-359, water-460 and water-439, are only found in the binary structure. Water-

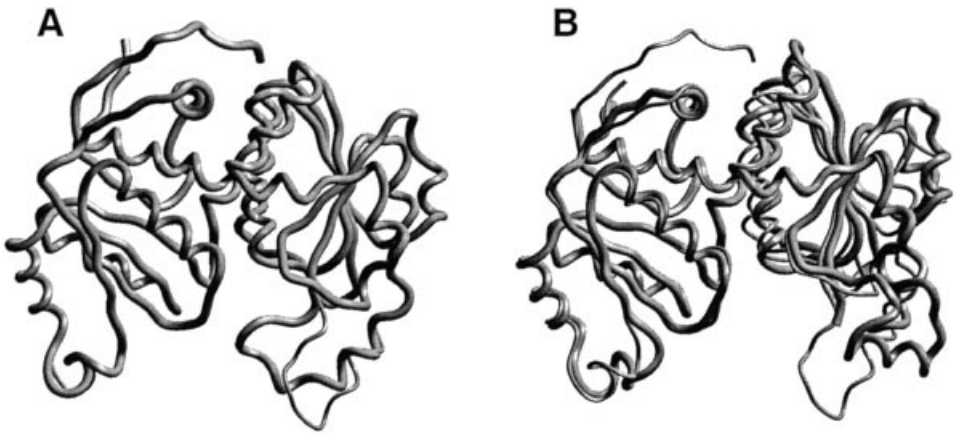

Figure 4 Conformational changes of OTCases in different liganded states

(**A**) Superposition of the PALO-replaced binary complex (thin trace) on to the ternary complex (thick trace; PDB code, 1oth), generated with 311 equivalent C^{α} coordinates excluding part of the SMG loop (residues 267–277). The RMSD between the structures is 0.36 Å. (**B**) Superposition of the PALO-replaced binary complex (thin trace) onto the *E. coli* apo-OTCase (thick trace; PDB code, 1akm) using the β-sheet core of the CP domain. Relative to the binary complex, the *E. coli* apo-OTCase has an interdomain angle that is 4.6° more open. The Figure was generated using the program SETOR [62].

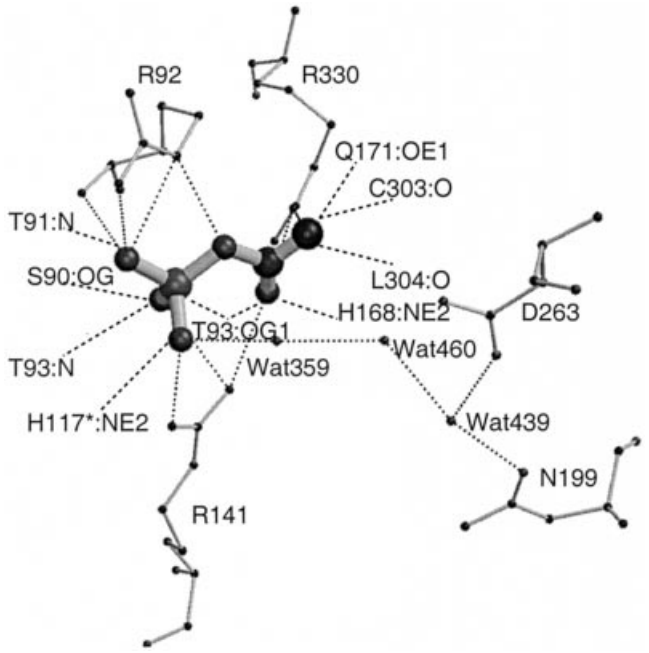

Figure 5 Schematic drawing showing the interactions of CP with active-site residues. CP is shown in bold

The residue indicated with an asterisk is from an adjacent subunit. Wat, water.

Table 2 Interactions between the protein and CP

Substrate atoms	Protein atoms (distance in Å)
CP:O1P	Arg^{141}:NH1 (2.71), His^{117}:NE2 (2.80)*
CP:O2P	Thr^{93}:N (2.84), Thr^{93}:OG1 (2.84), Ser^{90}:OG (2.67), Arg^{141}:NH2 (3.14)
CP:O3P	Thr^{91}:N (2.84), Arg^{92}:N (2.89), Arg^{92}:NE (2.98), Arg^{92}:NH2 (2.92)
CP:OA	Arg^{92}:NE (2.83)
CP:O1	Thr^{93}:OG1 (2.92), His^{168}:NE2(2.89), Arg^{141}:NH2 (2.92), Arg^{330}:NH1 (2.98)
CP:NP	Gln^{171}:OE1 (2.80), Cys^{303}:O (2.96), Leu^{304}:O (3.27), Arg^{330}:NH1 (3.23)

* His^{117} is from an adjacent subunit in the catalytic trimer.

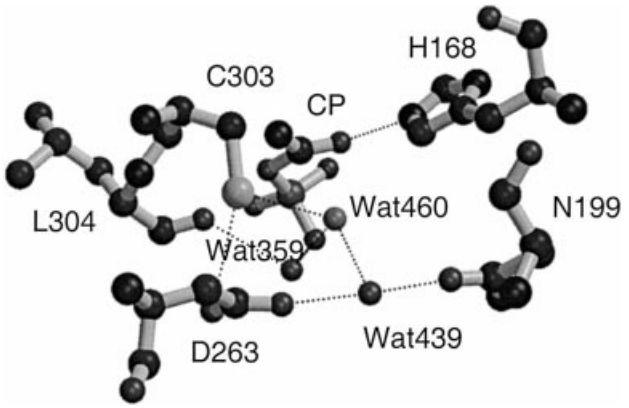

Figure 6 Putative metal binding site and surrounding residues. Water-460, located in the centre of S^{γ} of Cys^{303}, $C^{\delta 2}$ of His^{168}, water-359 and water-439, was proposed as a metal binding site

The Figure was generated using MOLSCRIPT [58] and Raster3D [59,60]. Wat, water.

359 hydrogen bonds to the one of the phosphate oxygen atoms (O1P) of CP (3.04 Å), the carbonyl oxygen of Leu^{304} (2.97 Å) and water-460 (3.05 Å). Water-460 hydrogen bonds to S^{γ} of Cys^{303} (3.16 Å), water-439 (2.93 Å) and water-359 (3.05 Å), and makes close contact with $C^{\delta 2}$ of His^{168} (3.47 Å). Water-439 hydrogen bonds to $O^{\delta 2}$ of Asp^{263} (2.81 Å), $O^{\delta 1}$ of Asn^{199} (3.09 Å) and water-460 (2.93 Å). These water molecules are important in maintaining the side chains of Asn^{199} and Asp^{263} in the correct conformations to bind the second substrate. In this extensive hydrogen network (Figure 6), water-460 is located in the centre of a tetrahedron consisting of water-359, water-439, S^{γ} of Cys^{303} and $C^{\delta 2}$ of His^{168}.

Table 3 Comparison of intersubunit interactions between the CP-liganded binary complex and the CP-L-norvaline-liganded ternary complex

Interaction	Distance (Å) in the binary complex	Distance (Å) in the ternary complex
Arg^{89}:NH1–Thr^{113}:O	2.57	2.53
Arg^{89}:NH1–Gln^{114}:O	3.32	–
Arg^{89}:NH1–Ile^{116}:O	3.00	2.80
Arg^{89}:NH1–Asn^{121}:OD1	3.31	–
Ser^{90}:N–Glu^{115}:O	2.91	2.84
Thr^{91}:OG1–His^{117}:N	2.92	3.07
Arg^{92}:NH1–Glu^{122}:OE1	2.72	2.71
Arg^{92}:NH1–Glu^{122}:OE2	3.36	3.41
Arg^{92}:NH2–Glu^{122}:OE1	3.41	3.31
Arg^{92}:NH2–Glu^{122}:OE2	2.82	2.73
Arg^{94}:NH2–Phe^{110}:O	2.68	2.83
Glu^{98}:OE2–His^{107}:NE2	2.75	2.80
Thr^{99}:OG1–Met^{134}:O	3.47	3.46
Gln^{114}:OE1–Gln^{114}:OE1	3.24	–
His^{117}:NE2–CP:O1P	3.33	2.80
His^{117}:NE2–CP:O2P	3.22	3.09
Val^{120}:O–Lys^{307}:NZ	2.67	–
Asp^{126}:OD1–Tyr^{317}:OH	2.90	3.06
Met^{134}:O–Lys^{331}:NZ	2.79	2.87

* Intersubunit interactions are defined as contacts of less than 3.5 Å which are able to make an electron donor–acceptor pair.

Rotation of the side chain of His^{168} by 180° around the C^{β}–C^{γ} bond will make $N^{\delta 1}$ of His^{168} hydrogen bond to water-460. The position of water-460 seems to be an ideal metal binding site for metal ions such as Zn(II) or Cd(II) [34,35].

Intersubunit interactions

The interfaces between the three subunits involve mainly the CP binding domains (Figure 2). As listed in Table 3, the residues that are involved in the intersubunit interactions come mainly from two regions, residues 89–99 and residues 113–134. Both regions contribute residues involved in binding the phosphate group of CP. As has been noted, the interactions between Arg^{92} and Glu^{122}, and between Arg^{94} and Phe^{110} are conserved in all OTCases and ATCases [8]. These interactions are likely to be important for maintaining the trimeric structure and the catalytic activity. Although residue 91 can be glycine, methionine or leucine, the interaction between $O^{\gamma 1}$ of Thr^{91} and the backbone N of His^{117} seems to have functional significance in regulating affinity for CP. Since there are no significant structural differences except for the differences in the position of the 'adjacent loop' and the SMG loop between the binary and ternary complex, most intersubunit interactions in the binary complex are also found in the ternary complexes. The only significant difference between the binary and ternary complex is the interaction between the backbone O of Val^{120} and N^{ζ} of Lys^{307}, found only in the binary complex as a result of the shift in the backbone of Val^{120}.

DISCUSSION

Domain closure

As shown in Figure 4, the binary and ternary structures are extremely similar except at the SMG loop and the 'adjacent' loop. The orientation of the two domains in the CP–OTCase structure described in the present study is very similar to that observed in PALO-liganded human OTCase and PALO-liganded *E. coli* OTCase and differs by 4–5° from the relative domain orientation of unliganded *E. coli* OTCase (Figure 4) [9]. This suggests that CP binding induces most of the domain reorientation that takes place during binding of the substrates, with binding of the second substrate, L-ornithine, only bringing the SMG loop into the active site. These results are consistent with earlier reports of crystal soaking experiments with *E. coli* OTCase in which CP cracked the unliganded crystals [36], and the difference ultraviolet absorption spectra of *E. coli* and yeast OTCases showing that CP binding alone produced the most significant spectral signal [17,37,38]. Recent ultraviolet spectroscopy experiments with human OTCase also demonstrate that binding of the first substrate, CP, induces a large protein isomerization [18].

There is an important caveat to this conclusion if only the PALO-replaced binary complex crystals are available, since the PALO-replaced binary complex was prepared by displacing PALO from crystals grown in its presence. It is possible that crystal packing forces maintain the domain orientation of the PALO-liganded crystals, and that in solution, the interdomain orientation of the binary complex is different. This question was resolved by determining the structure of a binary complex obtained by co-crystallization with CP. The interdomain angle in the CP-cocrystallized binary structure was less than 1° different from that in the PALO-replaced binary complex. Because the structure of human apo-OTCase is not available, the conclusion can only be made by comparison with the structure of other apo-OTCases. We have used the structure of the PALO-replaced binary complex as a reference point and calculated the relative interdomain angles using the β-sheet cores for all available apo-OTCase structures. Relative to the human binary structure, the interdomain angle is 3.3° more open in *Py. furiosus* OTCase, 4.6° more open in *E. coli* OTCase, and 11.6° more open in *Ps. aeruginosa* OTCase. The relative interdomain angle of human apo-OTCase is most likely to fall somewhere in the above range. Since all of the existing evidence, from both crystal structures and experiments in solution, for all of the OTCases that have been examined indicates that CP, rather than L-ornithine, induces domain movement, it appears unlikely that this is an artifact. The only transcarbamylase in which binding of the second substrate is known to be required to produce domain closure is *E. coli* ATCase. This enzyme is a dodecamer containing both catalytic and regulatory subunits, and domain closure is accompanied by a large change in quaternary structure (the T → R transition) [7]. It may be that binding of the second substrate is required for the large quaternary structure change, whereas binding of the first substrate is sufficient to promote domain closure in the absence of other subunit constraints. The crystal structures of the binary complexes of the catalytic subunit of *E. coli* ATCase will answer this question.

Substrate recognition

The conserved Ser-Thr-Arg-Thr-Arg (Ser^{90}-Thr^{91}-Arg^{92}-Thr^{93}-Arg^{94} in human OTCase) motif has long been recognized as the binding site for CP. The crystal structures of ATCase [39,40] and OTCase [10,13,14] indicate that this motif is involved in binding the phosphate group of CP. The Ser-Thr-Arg-Thr-Arg motif is located at the N-terminal end of helix 2, and the side chains of Ser^{90}, Thr^{93} and Arg^{92} are involved in direct interactions with CP (Table 2). The specific spatial arrangement of these residues and the presence of a positively charged arginine together with a dipole interaction of helix 2 make it an ideal site for binding the negatively charged phosphate group of CP. This Ser-Thr-Arg-Thr-Arg motif is also present in oxamate transcarbamylase (M.

Malamy, personal communication). Even *O*-carbamoyltransferase, which transfers a carbamoyl group from CP to an oxygen of a second substrate during the biosynthesis of some antibiotics, appears to have a similar binding motif for CP [41]. Whether or not this is a universal motif for binding CP requires further investigation. Even though Thr^{91} and Arg^{94} are not directly involved in binding CP, these two residues are functionally important. The side chain of Thr^{91} points outward from the active site and interacts with the backbone nitrogen of His^{117} from the adjacent subunit. This intersubunit interaction is important in assisting the side chain of His^{117} from the adjacent subunit in binding CP. In OTCases from sweet pea and *Ps. syringe* pv. *phaseolicola*, Thr^{91} is replaced by methionine and glycine respectively [42,43]. Both of these plant OTCases exhibit elevated K_m values for CP and reduced affinities for the bi-substrate analogue inhibitor, PALO, relative to other OTCases [44,45]. The relatively weak binding of CP to plant OTCases, relative to ATCases, may be important for partitioning CP between *de novo* pyrimidine and arginine biosynthesis, as a single glutamine-dependent CP synthetase provides the CP intermediate to both pathways [42]. The side chain of Arg^{94}, which interacts with the carbonyl oxygen of Phe^{110} from the adjacent subunit, may have a similar role.

His-Pro-Xaa-Gln (His^{168}-Pro^{169}-Xaa^{170}-Gln^{171} in human OTCase), which is involved in binding the carbamoyl group of CP, is the second conserved motif. Absolute conservation of this motif in the transcarbamylase family indicates that it is essential for enzyme function. Mutagenesis experiments in the ATCase indicate that this motif is involved mainly in polarizing the C–O bond of CP [46,47]. Similar roles for these residues are expected in the OTCase.

The conserved His-Cys-Leu-Pro (His^{302}-Cys^{303}-Leu^{304}-Pro^{305} in human OTCase) motif is part of the L-ornithine binding site [34,48]. Cys^{303} has been shown to be essential in binding the second substrate using mutagenesis and chemical modification [34,49,50]. Although the crystal structure does not provide direct evidence that the side chain of Cys^{303} is involved in binding, the N^{ϵ} atom of L-ornithine may interact with the S^{γ} of Cys^{303} [14]. The His-Cys-Leu-Pro motif in OTCase is replaced by His-Pro-Leu-Pro in *E. coli* ATCase. The His-Cys-Leu-Pro motif is also found in the sequence of oxamate transcarbamylase. Structural comparison between OTCase and ATCase indicates that the His-Xaa-Leu-Pro motifs in both enzymes are in similar conformations that allow the carbonyl oxygens of Cys^{303} and Leu^{304} to interact with the carbamoyl nitrogen of CP and the attacking nitrogen from the second substrate. The conserved His-Xaa-Leu-Pro motif probably stabilizes the tetrahedral intermediate, rather than being essential for binding the second substrate, since this motif has a very similar conformation in different transcarbamylases.

The available crystal structures clearly indicate that the conserved motif Asp-Xaa-Xaa-Xaa-Ser-Met-Gly (Asp^{263}-Xaa^{264}-Xaa^{265}-Xaa^{266}-Ser^{267}-Met^{268}-Gly^{269} in human OTCase) from the flexible SMG loop is the main binding site for L-ornithine in OTCase. The equivalent loop in ATCase is called the 240s loop and has the conserved Arg-Xaa-Gln-Xaa-Glu-Arg (Arg^{229}-Xaa^{230}-Gln^{231}-Xaa^{232}-Glu^{233}-Arg^{234} in *E. coli* ATCase) motif, which binds L-aspartate. The binding pocket for the second substrate is a typical induced-fit pocket, with binding of the second substrate inducing a conformational change, which brings the flexible loop into the active site. Similar conformational changes probably occur in other members of the transcarbamylase family, such as oxamate transcarbamylase. However, the Asp-Xaa-Xaa-Xaa-Ser-Met-Gly motif in OTCase is not a universal binding motif for L-ornithine binding. In other ornithine binding proteins, such as carbamoyl phosphate synthetase from *E. coli* [51], arginase from *Bacillus caldovelox* [52] and lysine/arginine/ornithine-binding protein from *Salmonella typhimurium* [53,54], the Asp-Xaa-Xaa-Xaa-Ser-Met-Gly motif is not found.

Flexibility of the SMG loop

Superposition of the binary and ternary complexes demonstrates that the SMG loop shifts by more than 8.0 Å when the second substrate binds (Figure 4). The high *B* factors associated with residues 266–279 in the binary structure indicate that this loop has a high degree of flexibility before the second substrate binds. Flexibility of the equivalent 240s loop in ATCase has been previously reported. The movement of this loop seems to be essential for binding the second substrate and releasing the products. Whether the movement of this loop is a common feature during the catalytic reaction in the transcarbamylase family remains to be established.

Putative metal binding site

Zn(II) and Cd(II) ions can bind tightly to the OTCase [34,35]. When the metal ion is added before CP, binding of L-ornithine becomes co-operative, perhaps as a result of an interaction with the cysteine residue in the active site [34,55,56]. However, when CP is added before the metal ion, Zn(II) acts as a classical, reversible, inhibitor.

The structure of the binary complex identifies a potential metal binding site which would be expected to have these characteristics (Figure 6). This site is formed by the side chains of Cys^{303} and two water molecules, which interact with the phosphate oxygen of CP, the carbonyl oxygen of Leu^{303}, the side chains of Asp^{263} and Asn^{199} and other water molecules when CP is present. The side chain of His^{168} is within interaction range of this metal site; however, when CP is present, the $N^{\epsilon 2}$ atom of His^{168} forms a strong hydrogen bond with the carbonyl oxygen of CP so that the side chain of His^{168} is not available as a ligand. When CP is absent, the side chain of His^{168} could bind Zn(II) via a slight conformational change. This model is consistent with previous observations of Zn(II) binding to OTCase: (1) active site Cys^{303} is involved in binding Zn(II) [34]; (2) Zn(II) occupies the position of L-ornithine, and will therefore compete with L-ornithine binding; (3) when CP is present, Zn(II) binding is weak, because the side chain of His^{168} is not available as a ligand; and (4) when CP is absent, the side chain of His^{168} will become one of the ligands. The strong interactions between Zn(II) and the residues from two domains will induce enzyme isomerization and, eventually, the Zn(II) will be trapped tightly in the active site and inactivate the enzyme.

Ordered binding of substrate

Kinetic studies predict ordered Bi Bi binding of substrates in both ATCase and OTCase, with CP binding first, L-aspartate or L-ornithine binding second, carbamoylaspartate or citrulline dissociating first, and phosphate dissociating last [38,57]. The structure of the binary complex provides a clear explanation for the ordered binding of substrates. CP binds in a deep pocket, and in the ternary complex, CP is completely buried by the second substrate and the SMG loop [14]. The CP binding site is more accessible in the binary structure, in which the position of the SMG is away from the active site. The structures clearly indicate that CP must bind first since binding of the second substrate closes the active site.

We thank Dr L. Banaszak for permitting our use of the diffraction equipment in the Kahlert Center for Structure Biology at the University of Minnesota. We also thank Dr M. Capel for his assistance during data collection at beamline X12B in the National Synchrotron Light Source at Brookhaven National Laboratory, U.S.A. This facility is supported by the United States Department of Energy Offices of Health and Environmental Research and of Energy Sciences, and by the National Science Foundation. Some calculations were carried out on the IBM SP machine at the Minnesota Supercomputer Center. We thank Drs G. Barany and D. Venugopal for synthesizing PALO. This work was supported by Public Health Service Grant DK-47870 from the National Institute of Diabetes, Digestive and Kidney Diseases (to M. T. and N. M. A.).

REFERENCES

1 Bojanowski, R., Gaudy, E., Valentine, R. C. and Wolfe, R. S. (1964) Oxamic transcarbamylase of *Streptococcus allantoicus*. J. Bacteriol. **57**, 75–80
2 Wauven, C. V., Simon, J., Slos, P. and Stalon, V. (1986) Control of enzyme synthesis in the oxalurate catabolic pathway of *Streptococcus faecalis* ATCC 11700: evidence for the existence of a third carbamate kinase. Arch. Microbiol. **145**, 386–390
3 Wargnies, B., Lauwers, N. and Stalon, V. (1979) Structure and properties of the putrescine carbamoyltransferase of *Streptococcus faecalis*. Eur. J. Biochem. **101**, 143–152
4 Tricot, C., de Coen, J. L., Momin, P., Falmagne, P. and Stalon, V. (1989) Evolutionary relationships among bacterial carbamoyltransferases. J. Gen. Microbiol. **135**, 2453–2464
5 Hommes, F. A., Eller, A. G., Scott, D. F. and Carter, A. L. (1983) Separation of ornithine and lysine activities of the ornithine-transcarbamylase-catalyzed reaction. Enzyme **29**, 271–277
6 Carter, A. L., Eller, A. G., Rufo, S., Metoki, K. and Hommes, F. A. (1984) Further evidence for a separate enzymic entity for the synthesis of homocitrulline, distinct from the regular ornithine transcarbamylase. Enzyme **32**, 26–36
7 Lipscomb, W. N. (1994) Aspartate transcarbamylase from *Escherichia coli*: activity and regulation. Adv. Enzymol. Relat. Areas Mol. Biol. **68**, 67–151
8 Allewell, N. M., Shi, D., Morizono, H. and Tuchman, M. (1999) Molecular recognition by ornithine and aspartate transcarbamylase. Acc. Chem. Res. **32**, 885–894
9 Jin, L., Seaton, B. A. and Head, J. F. (1997) Crystal structure at 2.8 Å resolution of anabolic ornithine transcarbamylase from *Escherichia coli*. Nat. Struct. Biol. **4**, 622–625
10 Ha, Y., McCann, M. T., Tuchman, M. and Allewell, N. M. (1997) Substrate-induced conformational change in a trimeric ornithine transcarbamoylase. Proc. Natl. Acad. Sci. U.S.A. **94**, 9550–9555
11 Villeret, V., Tricot, C., Stalon, V. and Dideberg, O. (1995) Crystal structure of *Pseudomonas aeruginosa* catabolic ornithine transcarbamoylase at 3.0 Å resolution: a different oligomeric organization in the transcarbamoylase family. Proc. Natl. Acad. Sci. U.S.A. **92**, 10762–10766
12 Villeret, V., Clantin, B., Tricot, C., Legrain, C., Roovers, M., Stalon, V., Glansdorff, N. and van Beeumen, J. (1998) The crystal structure of *Pyrococcus furiosus* ornithine carbamoyltransferase reveals a key role for oligomerization in enzyme stability at extreme high temperature. Proc. Natl. Acad. Sci. U.S.A. **95**, 2801–2806
13 Shi, D., Morizono, H., Ha, Y., Aoyagi, M., Tuchman, M. and Allewell, N. M. (1998) 1.85 Å resolution crystal structure of human ornithine transcarbamoylase complexed with *N*-phosphonacetyl-L-ornithine. J. Biol. Chem. **273**, 34247–34254
14 Shi, D., Morizono, H., Aoyagi, M., Tuchman, M. and Allewell, N. M. (2000) Crystal structure of human ornithine transcarbamylase complexed with carbamoyl phosphate and L-norvaline at 1.9 Å resolution. Proteins: Struct. Funct. Genet. **39**, 271–277
15 Baur, H., Stalon, V., Falmagne, P., Luthi, E. and Haas, D. (1987) Primary and quaternary structure of the catabolic ornithine carbamoyltransferase from *Pseudomonas aeruginosa*. Extensive sequence homology with the anabolic ornithine carbamoyltransferases of *Escherichia coli*. Eur. J. Biochem. **166**, 111–117
16 Ke, H., Lipscomb, W. N., Cho, Y. and Honzatko, R. (1988) Complex of *N*-phosphonacetyl-L-aspartate with aspartate carbamoyltransferase. J. Mol. Biol. **204**, 725–747
17 Miller, A. W. and Kuo, L. C. (1990) Ligand-induced isomerization of *Escherichia coli* ornithine transcarbamoylase. An ultraviolet difference analysis. J. Biol. Chem. **265**, 15023–15027
18 de Gregorio, A., Risitano, A., Capo, C., Crinio, C., Petruzzelli, R. and Desideri, A. (1999) Evidence of carbamoylphosphate induced conformational changes upon binding to human ornithine carbamoyltransferase. Biochem. Mol. Biol. Int. **47**, 965–970
19 Knier, B. and Allewell, N. M. (1978) Calorimetric analysis of aspartate transcarbamylase from *Escherichia coli*: Binding of substrates and substrate analogs to the native enzyme and catalytic subunit. Biochemistry **17**, 784–790
20 Morizono, H., Tuchman, M., Rajagopal, B. S., McCann, M. T., Listrom, C. D., Yuan, X., Venugopal, D., Barany, G. and Allewell, N. M. (1997) Expression, purification and kinetic characterization of wild-type human ornithine transcarbamylase and a recurrent mutant that produces 'late onset' hyperammonaemia. Biochem. J. **322**, 625–631
21 Howard, A. J., Gilliland, G. L., Finzel, B. C., Poulos, T. L., Olendorf, D. H. and Scalemme, F. R. (1987) The use of an imaging proportional counter in macromolecular crystallography. J. Appl. Crystallogr. **20**, 383–387
22 Otwinowski, Z. and Minor, W. (1997) Processing of X-ray diffraction data collected in oscillation mode. Methods Enzymol. **276**, 307–326
23 Jones, T. A., Zou, J. Y., Cowan, S. W. and Kjeldgaard, M. (1991) Improved methods for building protein models in electron density maps and location of errors in these models. Acta Crystallogr. Sect A: Found Crystallogr. **47**, 110–119
24 Brünger, A. T. (1996) X-PLOR v3.8, Yale University Press, New Haven, U.S.A.
25 Jiang, J.-S. and Brünger, A. T. (1994) Protein hydration observed by X-ray diffraction. J. Mol. Biol. **243**, 100–115
26 Collaborative Computer Project, Number 4. (1994) The CCP4 suite: programs for protein crystallography. Acta. Cryst. D **50**, 760–763
27 Brünger, A. T. (1992) Free R value: a novel statistical quantity for assessing the accuracy of crystal structures. Nature (London) **355**, 472–475
28 Laskowski, R. A., MacArthur, M. W., Moss, D. S. and Thornton, J. M. (1993) PROCHECK-A program to check the stereochemical quality of protein structures. J. Appl. Crystallogr. **26**, 283–291
29 Tong, L. (1993) REPLACE, a suite of computer programs for molecular-replacement calculation. J. Appl. Crystallogr. **26**, 748–751
30 Tong, L. (1996) Combined molecular replacement. Acta Crystallogr. Sect. A: Found. Crystallogr. **52**, 782–784
31 Brünger, A. T., Adams, P. D., Clore, G. M., DeLano, W. L., Gros, P., Crosse-Kunstleve, R. W., Jiang, J. S., Kuszewski, J., Nilges, M., Pannu, N. S. et al. (1998) Crystallography & NMR System: A new software suite for macromolecular structure determination. Acta Crystallogr. Sect D: Biol. Crystallogr. **54**, 905–921
32 Hutchinson, E. G. and Thornton, J. M. (1996) PROMOTIF–A program to identify and analyze structural motifs in proteins. Protein Sci. **5**, 212–220
33 Valentini, G., de Gregorio, A., Di Salvo, C., Grimm, R., Bellocco, E., Cuzzocrea, G. and Iadarola, P. (1996) An essential lysine in the substrate-binding site of ornithine carbamoyltransferase. Eur. J. Biochem. **239**, 397–402
34 Kuo, L. C., Caron, C., Lee, S. and Herzberg, W. (1990) Zn^{2+} regulation of ornithine transcarbamoylase. II. Metal binding site. J. Mol. Biol. **211**, 271–280
35 Aoki, Y., Sunaga, H. and Suzuki, K. T. (1988) A cadmium-binding protein in rat liver identified as ornithine carbamoyltransferase. Biochem. J. **250**, 735–742
36 Kuo, L. C. and Seaton, B. A. (1989) X-ray diffraction analysis on single crystals of recombinant *Escherichia coli* ornithine transcarbamoylase. J. Biol. Chem. **264**, 16246–16248
37 Legrain, C. and Stalon, V. (1976) Ornithine carbamoyltransferase from *Escherichia coli*: purification, structure and steady-state kinetic analysis. Eur. J. Biochem. **63**, 289–301
38 Goldsmith, J. D. and Kuo, L. C. (1993) Utilization of conformational flexibility in enzyme activities-linkage between binding isomerization and catalysis. J. Biol. Chem. **268**, 18481–18484
39 Gouaux, J. E. and Lipscomb, W. N. (1990) Crystal structures of phosphonacetamide ligated T and phosphonacetamide and malonate ligated R states of aspartate carbamoyltransferase at 2.8 Å resolution and neutral pH. Biochemistry **29**, 389–402
40 Gouaux, J. E. and Lipscomb, W. N. (1988) Three-dimensional structure of carbamoyl phosphate and succinate bound to aspartate carbamoyltransferase. Proc. Natl. Acad. Sci. U.S.A. **85**, 4205–4208
41 Coque, J. J. R., Perea-Llarena, F. J., Enguita, F. J., Fuente, J. L., Martin, J. F. and Liras, P. (1995) Characterization of the *cmcH* genes of *Nocardia lactamdurans* and *Streptomyces clavuligerus* encoding a functional 3′-hydroxymethylcephem *O*-carbamoyltransferase for cephamycin biosynthesis. Gene **162**, 21–27
42 Williamson, C. L., Lake, M. R. and Slocum, R. D. (1996) Isolation and characterization of a cDNA encoding a pea ornithine transcarbamoylase (*argF*) and comparison with other transcarbamoylases. Plant Mol. Biol. **31**, 1087–1092
43 Mosqueda, G., Van den Broek, G., Saucedo, O., Bailey, A. M., Alvarez-Morales, A. and Herrera-Estrella, L. (1990) Isolation and characterization of the gene from *Pseudomonas syringae* pv. *phaseolicola* encoding the phaseolotoxin-insensitive ornithine carbamoyltransferase. Mol. Gen. Genet. **222**, 461–466
44 deRuiter, H. and Kolloffel, C. (1985) Properties of ornithine carbamoyltransferase from *Pisum sativum* L. Plant Physiol. **77**, 695–699
45 Templeton, M. D., Sullivan, P. A. and Shepherd, M. G. (1986) Phaseolotoxin-insensitive L-ornithine transcarbamoylase from *Pseudomonas syringae* pv. *phaseolicola*. Physiol. Mol. Plant Pathol. **29**, 393–403
46 Robey, E. A., Wente, S. R., Markby, D. W., Flint, A., Yang, Y. R. and Schachman, H. K. (1986) Effect of amino acid substitutions on the catalytic and regulatory properties of aspartate transcarbamoylase. Proc. Natl. Acad. Sci. U.S.A. **83**, 5934–5938

47 Stebbins, J. W., Xu, W. and Kantrowitz, E. R. (1989) Three residues involved in binding and catalysis in the carbamoyl phosphate binding site of *Escherichia coli* aspartate transcarbamylase. Biochemistry **28**, 2592–2600
48 Kraus, J. P., Hodges, P. E., Williamson, C. L., Horwich, A. L., Kalousek, F., Williams, K. P. and Rosenberg, L. E. (1985) A cDNA clone for the precursor of rat mitochondrial ornithine transcarbamylase: comparison of rat and human leader sequences and conservation of catalytic sites. Nucleic Acids Res. **13**, 943–952
49 McDowall, S., van Heeswijck, R. and Hoogenraad, N. (1990) Site-directed mutagenesis of Arg60 and Cys271 in ornithine transcarbamylase from rat liver. Protein Eng. **4**, 73–77
50 Marshell, M. and Cohen, P. P. (1980) The essential sulfhydryl group of ornithine transcarbamylase. J. Biol. Chem. **255**, 7296–7300
51 Thoden, J. B., Holden, H. M, Wesenberg, G., Raushel, F. M. and Rayment, I. (1997) Structure of carbamoyl phosphate synthetase: A journey of 96 Å from substrate to product. Biochemistry **36**, 6305–6316
52 Bewley, M. C., Jeffrey, P. D., Patchett, M. L., Kanyo, Z. F. and Baker, E. N. (1999) Crystal structures of *Bacillus caldovelox* arginase in complex with substrate and inhibitors reveal new insights into activation, inhibition and catalysis in the arginase superfamily. Structure (London) **7**, 435–448
53 Oh, R.-H., Pendit, J., Kang, C.-H., Nikaido, K., Gokeen, S., Ames, G. F.-L. and Kim, S.-H. (1993) Three-dimensional structures of the periplasmic lysine/arginine/ornithine-binding protein with and without a ligand. J. Biol. Chem. **268**, 11348–11355
54 Oh, R.-H., Ames, G. F.-L. and Kim, S.-H. (1994) Structural basis for multiple ligand specificity of the periplasmic lysine-, arginine-, ornithine-binding protein. J. Biol. Chem. **269**, 26323–26330
55 Kuo, L. C., Lipscomb, W. N. and Kantrowitz, E. R. (1982) Zn(II)-induced cooperativity of *Escherichia coli* ornithine transcarbamoylase. Proc. Natl. Acad. Sci. U.S.A. **79**, 2250–2254
56 Lee, S., Shen, W. H., Miller, A. W. and Kuo, L. C. (1990) Zn^{2+} regulation of ornithine transcarbamoylase. I. Mechanism of action. J. Mol. Biol. **211**, 255–269
57 Porter, R. W., Modebe, M. O. and Stark, G. R. (1969) Aspartate transcarbamylase: kinetic studies of the catalytic subunit. J. Biol. Chem. **244**, 1846–1859
58 Kraulis, P. J. (1991) MOLSCRIPT–A program to produce both detailed and schematic plots of protein structures. J. Appl. Crystallogr. **24**, 946–950
59 Bacon, D. J. and Anderson, W. F. (1988) A fast algorithm for rendering space-filling molecule picture. J. Mol. Graphics **6**, 219–220
60 Merrit, E. A. and Murphy, M. E. P. (1994) Raster3D Version 2.0–a program for photorealistic molecular graphics. Acta Crystallogr. Sect. D: Biol. Crystallogr. **50**, 869–873
61 Barton, G. L. (1993) ALSCRIPT: a tool to format multiple sequence alignments. Protein Eng. **6**, 37–40
62 Evans, S. V. (1993) SETOR: Hardware lighted three-dimensional solid model representations of macromolecules. J. Mol. Graphics **11**, 134–138

Received 17 May 2000/29 November 2000; accepted 9 January 2001